A new route to produce ^{52g}Mn with high purity for MultiModal Imaging

Mario Pietro Carante[1,2*], *Francesca* Barbaro[1,3], *Luciano* Canton[3], *Alessandro* Colombi[1,2], and *Andrea* Fontana[2]

[1]Università di Pavia, Dipartimento di Fisica, 27100 Pavia, Italy
[2]INFN (Istituto Nazionale di Fisica Nucleare), Sezione di Pavia, 27100 Pavia, Italy
[3]INFN (Istituto Nazionale di Fisica Nucleare), Sezione di Padova, 35131 Padova, Italy

Abstract. The ^{52g}Mn radionuclide is suitable for the innovative MultiModal Imaging technique, and in particular for a PET/MRI scan, due to its physical properties. The standard cyclotron-based production of ^{52g}Mn relies on the nuclear reaction ^{Nat}Cr(p,x)^{52g}Mn, but we have investigated theoretically the possibility of an alternative and competitive route, the reaction ^{Nat}V(α,x)^{52g}Mn, which has not been considered for this purpose so far. By using the nuclear reaction code TALYS, we found some discrepancies between the theoretical calculations of the cross sections and the corresponding experimental data. Therefore we tuned the parameters governing the nuclear level densities in the microscopic models implemented in TALYS, thus improving the agreement with the data. Then, by studying the cross sections for ^{52g}Mn and its contaminants, we have identified an optimal energy window for the production of high purity ^{52g}Mn, around 40 MeV. We have also calculated the time evolution of the number of nuclei of the different Mn isotopes, for an irradiation in this energy window, finding that this route is expected to lead to a higher yield and Radionuclidic Purity with respect to the standard reaction with ^{Nat}Cr. The study suggests the reaction ^{Nat}V(α,x)^{52g}Mn as a promising alternative route for the production of ^{52g}Mn.

1 Introduction

MultiModal Imaging is an innovative diagnostic technique consisting in the combination of two different diagnostic exams, based on different physical processes. An example is represented by the combination of Positron Emission Tomography (PET) and Magnetic Resonance Imaging (MRI), performed simultaneously by using a singular molecular agent. The radionuclide ^{52g}Mn appears of particular interest for this purpose because of its physical properties: it decays by the emission of a positron with energy of about 0.6 MeV, suitable to perform PET with good spatial resolution [1], and it has paramagnetic properties, which make it suitable for MRI. Moreover, its relatively long half-life of about 5.6 days is suitable for the radiolabeling of antibodies and other slow biological compounds for the study of pharmacokinetics.

* Corresponding author: mariopietro.carante@unipv.it

© The Authors, published by EDP Sciences. This is an open access article distributed under the terms of the Creative Commons Attribution License 4.0 (http://creativecommons.org/licenses/by/4.0/).

The standard cyclotron-based production route of ^{52g}Mn relies on the nuclear reaction ^{Nat}Cr(p,x)^{52g}Mn, which leads to the co-production of long-lived contaminants ^{53}Mn and ^{54}Mn: the latter in particular is the most important contaminant in view of clinical applications. Indeed, ^{48}Mn, ^{49}Mn, ^{50}Mn, ^{51}Mn and ^{52m}Mn have half-lives smaller than 1 h, and their contamination, if any, is thus negligible after a few hours. On the other hand, ^{55}Mn, which is stable, and ^{53}Mn, whose half-life is of about $3.7 \cdot 10^6$ years, cannot release a significant dose to the patient. Finally ^{54}Mn, with an intermediate half-life of 312 days, could represent an issue in terms of the expected dose increase to the patient [1]. A possible solution to limit the co-production of these contaminants is represented by the use of highly enriched targets of ^{52}Cr, by means of the reaction ^{52}Cr(p,n)^{52g}Mn, with a concomitant significant cost increase.

In [2], the reaction ^{Nat}V(α,x)^{52g}Mn was identified as a possible alternative route for the production of ^{52g}Mn. Through the use of state-of-art nuclear reaction codes, like TALYS [3], FLUKA [4] and EMPIRE [5], this reaction was shown to lead to a favourable yield of ^{52g}Mn, compared with the standard reaction with ^{Nat}Cr, in combination with a significantly lower production of ^{54}Mn. Nevertheless, the study pointed out that the experimental data available in the literature on the cross section of that reaction are very scattered, and that the standard simulations with the considered nuclear reaction codes cannot reproduce adequately the experimental data. On the other hand, standard TALYS calculations describe the cross section of the routine reaction ^{Nat}Cr(p,x)^{52g}Mn in agreement with the body of experimental data.

In view of possible applications of ^{52g}Mn to medical imaging, in the present work, in the framework of the METRICS project at INFN-LNL, we optimized some parameters of the TALYS code, in order to obtain a better agreement with the experimental measurements for the cross section of the ^{Nat}V reaction and to be able to obtain reliable predictions about the yield and purity of ^{52g}Mn if produced through this alternative reaction route.

2 Methods

In order to perform theoretical calculations of the cross sections for the production of the medical radionuclide of interest, we used modern nuclear reaction codes: in this work we focused in particular on the TALYS simulation package, which is actively developed and maintained. In TALYS, the evaluated nuclear reaction rates are based on the Hauser-Fesbach model [6] for the equilibrium mechanisms and on four different theoretical frameworks for the pre-equilibrium process. Moreover, there are six possible options for the description of the level density, ranging from the Fermi gas model to microscopic approaches. A total of 24 model combinations are thus available.

In a previous work [2] we decided not to select one particular model for level density and pre-equilibrium, but to deal with the theoretical variability provided by the different models. In particular, we introduced for each energy a Best Theoretical Evaluation (BTE) of the cross section, defined as the average between the first and the third quartile. Nevertheless, none of the 24 TALYS models, as well as the BTE, were able to reproduce adequately the experimental data for the cross section of the reaction ^{Nat}V(α,x)^{52g}Mn.

In this work, with the aim of improving the theoretical description of this cross section, we tuned some parameters of the TALYS code. More specifically, we selected, for the optical model, the so-called JLM (Jeukenne-Lejeune-Mahaux) semi-microscopic nucleon-nucleus spherical optical model potential [7] and, for the nuclear level density, we focused on the microscopic approach denoted as Hartree-Fock Models (HFM), specifically the temperature-dependent Hartree-Fock-Bogoliubov model with the tabulation from Hilaire's combinatorial tables [8] (TALYS option: *ldmodel* 6). The tabulated values can be rescaled by using two parameters (c and p), which modulate the HFM level densities according to the transformation:

$$\rho(E) = \exp(c\sqrt{E-p})\rho_{HFM}(E-p) \quad (1)$$

Parameters c and p represent a normalization and an energy shift, respectively. In the present work, we tuned these two parameters, thus modifying the original HFM level densities, in order to obtain theoretical calculations in agreement with the experimental cross sections, for the involved radionuclides. As a first step we performed a gross search, by varying c and p on a grid with a trial and error approach, until the achievement of a first qualitative agreement between theory and measurements. As a second step, we evaluated a global chi-square of all the involved cross sections and we performed a Minuit-based chi-square minimization procedure [9], by using c and p as free parameters, with initial values identified by the previous grid search. These two steps are described in detail in [10]. The computation of reliable cross sections allowed us to identify a promising energy window for the production of the radionuclide of interest with high yield and purity.

We also developed a tool, described in [2], to simulate an irradiation in this energy window and to evaluate the production yield of the radionuclide of interest and of its contaminants, as well as the Isotopic and Radio-Nuclidic Purities (IP and RNP), defined for this specific case respectively as:

$$IP = \frac{n_{52g_{Mn}}}{\sum_i n_{i_{Mn}}} \quad (2)$$

$$RNP = \frac{A_{52g_{Mn}}}{\sum_i A_{i_{Mn}}} \quad (3)$$

where n denotes the number of nuclei and A denotes the activity. These quantities are calculated by computing the production rate of each radionuclide and by solving standard Bateman equations for the radioactive isotopes, as described in [2].

3 Results

Focusing on the cross section of the reaction $^{Nat}V(\alpha,x)^{52g}Mn$, we found that the values c=0.4 and p=-1.0 for the level density of ^{52}Mn led to a minimization of the chi-square, as described in the Methods Section. Since the experimental data are extremely scattered and the different sets of data are not in agreement one each other within their uncertainties, the reduced chi-square assumes a very large value. Nonetheless, the chi-square minimization procedure led us to obtain a good overall agreement between the calculated cross section and the body of the experimental data [11-20]. This agreement is much better than for the BTE, calculated in [2]. The experimental data, the cross section obtained with the optimized c and p values and the BTE are reported in Fig. 1.

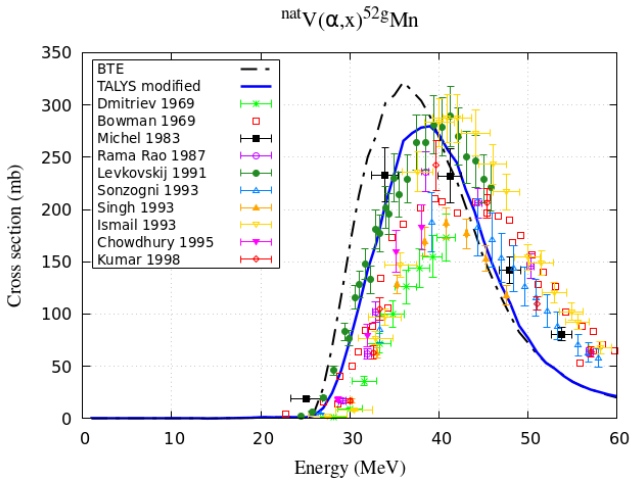

Fig. 1. Experimental data for the cross section of the reaction $^{Nat}V(\alpha,x)^{52g}Mn$, together with the optimized TALYS calculation (indicated TALYS modified) and with the BTE.

This same parameter set led also to a good agreement with the experimental data [15-17, 19-24] for the cross section of ^{54}Mn (Fig. 2), without the need to modify the default c and p values for this radionuclide. A correct description of the cross section of ^{54}Mn is fundamental, since it represents the main contaminant of ^{52g}Mn in the context of medical applications, due to its long half-life (about 312 days).

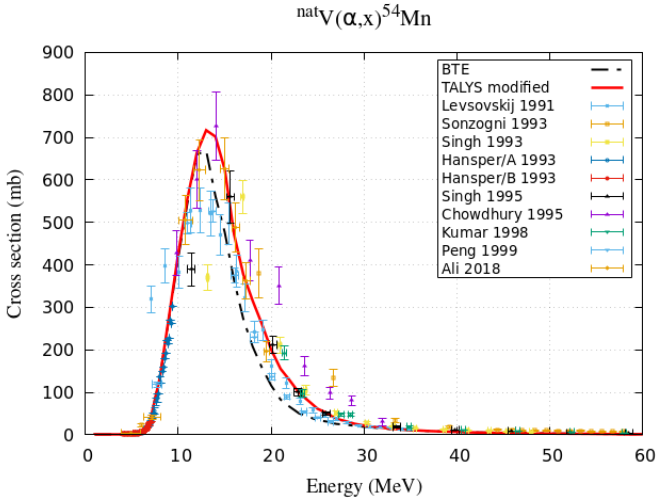

Fig. 2. Experimental and theoretical (BTE and TALYS modified) cross sections for the reaction $^{Nat}V(\alpha,x)^{54}Mn$.

After obtaining reliable theoretical cross sections, in agreement with the experimental data, for both ^{52g}Mn and ^{54}Mn, it is possible to identify a promising energy window to maximize the production of the radionuclide of interest, ^{52g}Mn, and to minimize the production of its main contaminant, ^{54}Mn, as shown in Fig. 3. More specifically, we considered the ratio between the cross section of ^{52g}Mn and the cross sections of all produced Mn isotopes: this ratio reaches its maximum at about 41 MeV. The width of the energy

window should correspond to a realistic target thickness: in this case we chose a thickness of 200 μm, as done in [2]. This energy window thus falls between about 34 and 48 MeV.

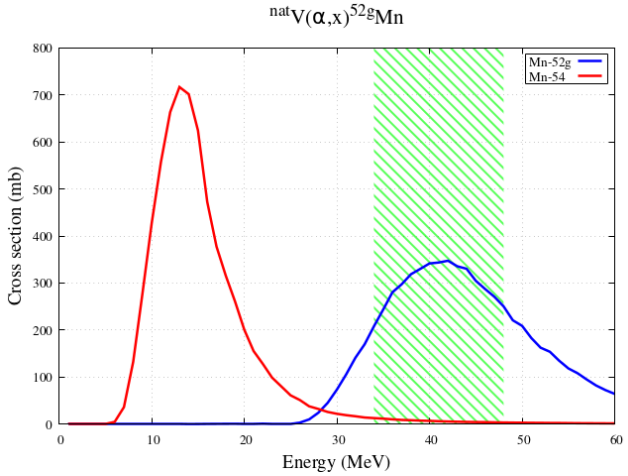

Fig. 3. Comparison between the optimized cross sections of ^{52g}Mn and ^{54}Mn, and identification of a promising energy window for the production of high purity ^{52g}Mn

In order to calculate the expected yields of the radionuclide of interest, ^{52g}Mn, and of its main contaminant, ^{54}Mn, we simulated an irradiation with beam current of 1 μA, irradiation time of 1 h, incident energy of 48 MeV and target thickness of 200 μm (corresponding to an output energy of 33.9 MeV). The results in terms of thick target yield (MBq/μAh) are reported in Table 1.

To compare these results with the standard production route, we also considered the reaction with protons on ^{Nat}Cr, for which the experimental cross section for the production of ^{52g}Mn can be adequately reproduced by standard TALYS calculations, as reported in [2]. Also for the case of ^{Nat}Cr we simulated an irradiation with the same conditions: beam current of 1 μA, irradiation time of 1 h and target thickness of 200 μm. In order to optimize the production of ^{52g}Mn also for this specific case, the incident energy of the protons was equal to 17 MeV, corresponding to an output energy of 14 MeV. The results in terms of physical thick target yield are reported in Table 1, in order to allow a direct comparison with the alternative reaction with ^{Nat}V.

Interestingly, the reaction with ^{Nat}V is expected to lead to a higher yield of ^{52g}Mn than the routine reaction with ^{Nat}Cr, with an associated lower production of the main contaminant ^{54}Mn. These results corroborate the idea of considering the $^{Nat}V(\alpha,x)^{52g}Mn$ reaction as a promising alternative route for the production of ^{52g}Mn.

Table 1. Physical thick target yields for both ^{52g}Mn and ^{54}Mn, produced by the reactions on ^{Nat}V and on ^{Nat}Cr.

Reaction	Physical thick target yield (MBq/μAh)
$^{Nat}V(\alpha,x)^{52g}Mn$	5.16 ± 1.04
$^{Nat}Cr(p,x)^{52g}Mn$	4.40 ± 0.51
$^{Nat}V(\alpha,x)^{54}Mn$	2.71 ± 0.22
$^{Nat}Cr(p,x)^{54}Mn$	4.89 ± 0.07

This idea is also strengthened by the expected RNP for the two considered reactions. Indeed, we determined the time evolution of the produced activities for both the nuclide of

interest and all its contaminants, and we calculated the RNP, which was found to be higher for the ^{Nat}V reaction than for the ^{Nat}Cr one, as shown in Fig. 4. It is important to point out that the RNP for ^{Nat}V may be affected by the uncertainties related to the c and p values obtained for ^{52g}Mn cross section. However, the curve presented in Fig. 4 is a reasonable estimate, since it is deduced from cross sections in agreement with the experimental data. In any case, in order to obtain a more accurate RNP, it would be essential to have more precise experimental data for a more accurate calibration of the model parameters.

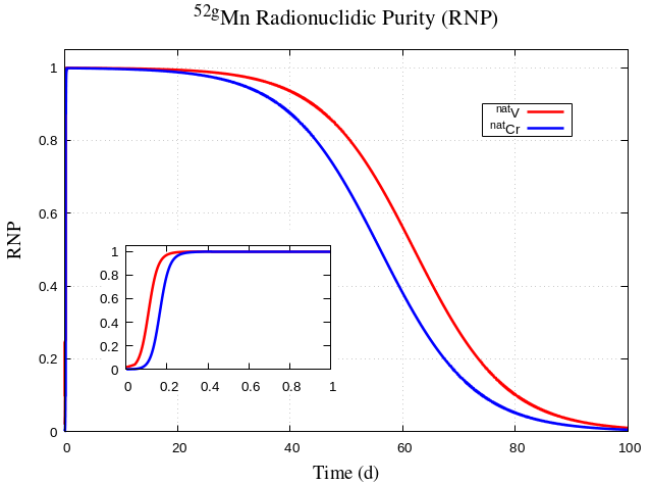

Fig. 4. Comparison between the Radionuclidic Purities of ^{52g}Mn for the two reactions with ^{Nat}V and ^{Nat}Cr, for 1 μA beam current, 1 h irradiation time and 200 μm target thickness. The inset shows the evolution for the first 24 h, including the irradiation time.

4 Conclusions

In the present work we considered the reaction ^{Nat}V(α,x)^{52g}Mn, as an alternative route to the standard reaction with protons on ^{Nat}Cr, to produce ^{52g}Mn with high purity in view of MultiModal Imaging applications. As a first step we tuned the parameters governing the level density description in a microscopic model implemented in the TALYS nuclear reaction code, in order to find a good agreement between theoretical calculations and experimental data available in the literature. This procedure was performed for both the radionuclide of interest, ^{52g}Mn, and its contaminants, mainly focusing on ^{54}Mn. A promising energy window to maximize the production of ^{52g}Mn with respect to the contaminants was thus identified by analysing the cross sections, and a virtual irradiation was simulated with an appropriate beam energy. The results of this calculation show that the reaction with ^{Nat}V is expected to lead to a higher yield of ^{52g}Mn compared to the standard ^{Nat}Cr reaction, with an associated lower production of the main contaminant, ^{54}Mn. The RadioNuclidic Purity of ^{52g}Mn is also expected to be higher for the ^{Nat}V reaction. These calculations support the idea of considering the ^{Nat}V(α,x)^{52g}Mn reaction as a promising alternative route for the production of ^{52g}Mn for medical applications. Nevertheless, it is important to observe that, whereas the production with ^{Nat}Cr can be achieved with hospital cyclotrons exploiting low energy protons, the ^{Nat}V reaction requires 40-MeV alpha particles, only available in advanced research centers. For these centers, however, the new production route may be considered as a valuable alternative, also considering that the half-life of ^{52g}Mn would allow for a relatively long-distance redistribution.

References

1. M. Brandt, J. Cardinale, I. Rausch, T.L. Mindt, J. Label Compd. Radiopharm. **62**, 8 (2019)
2. A. Colombi, M.P. Carante, F. Barbaro, L. Canton, A. Fontana, Nucl. Technol., DOI: 10.1080/00295450.2021.1947122 (2021)
3. S. Goriely, S. Hilaire, A.J. Koning, Astron. Astrophys. **487**, 2 (2008)
4. Battistoni et al., AIP Conf. Proc. **896**, 31 (2006)
5. M. Herman et al., Nucl. Data Sheets, **108**, 12 (2007)
6. W. Hauser, H. Feshbach, Phys. Rev., **87**, 2 (1952)
7. E. Bauge, J.P. Delaroche, M. Girod, Phys. Rev. C, **63** (2001)
8. S. Hilaire, M. Girod, S. Goriely, A.J. Koning, Phys. Rev. C, **86** (2012)
9. F. James, M. Roos, Comput. Phys. Commun., **10**, 343 (1975)
10. F. Barbaro, L. Canton, M.P. Carante, A. Colombi, L. De Dominicis, A. Fontana, F. Haddad, L. Mou, G. Pupillo, Phys. Rev. C, **104**, 044619 (2021)
11. P.P. Dimitriev, I.O. Constantinov, N.N. Krasnov, At. Energy, **26**, 5 (1969)
12. W.W. Bowman, M. BLANN, Nucl. Phys. A, **131**, 3 (1969)
13. R. Michel, G. Brinkmann, R. Stück, Nucl. Data Sci. Tech (Ed. Springer, Dordrecht, 1983)
14. J.R. Rao et al., J. Phys. G., **13**, 4 (1987)
15. V.N. Levkovskij, Cross-Section of Medium Mass Nuclide Activation (A = 40–100) by Medium Energy Protons and AlphaParticles (E = 10–50 MeV), Intervesi, Moskow, Russia, (1991)
16. A.A. Sonzogni et al., J. Radioanal. Nucl. Chem., **170**, 1 (1993)
17. N.L. Singh, S. Agarwal, J.R. Rao, Can. J. Phys., **71**, 3-4 (1993)
18. M. Ismail, Pramana, **40**, 3 (1993)
19. D.P. Chowdhury et al., Nucl. Instrum. Meth. Phys. Res. B, **103**, 3 (1995)
20. B. Bindu Kumar, S. Mukherjee, N.L. Singh, Phys. Scr., **57**, 2 (1998)
21. V.Y. Hansper et al., Nucl. Phys. A, **551**, 1 (1993)
22. N.L. Singh et al., J. Phys. G, **21**, 3 (1995)
23. X. Peng, F. He, X. Long, Nucl. Instrum. Meth. Phys. Res. B, **152**, 4 (1999)
24. B. Ali et al., Pramana – J. Phys., **90**, 3 (2018)